

Introduction

Quantitative interpretation (QI) is routinely applied to conventional reservoirs, with steps such as rock physics modelling (RPM), fluid substitution and inversion into elastic properties being firmly established in the geophysical workflow deployed in the successful development of hydrocarbon reserves (see for example, Simm and Bacon, 2014). For unconventional reservoirs, QI is equally valuable, but has not seen the same take up, perhaps due to lower development and drilling costs associated with land based assets. However, QI for unconventional reservoirs is a cause that we are championing here.

Arguably, the principal parameter in characterizing an unconventional reservoir is the total organic carbon (TOC) concentration (Vernik, 2016), with its quantification a key to screening reserves for potential development. A QI workflow for low permeability shale reservoirs can be exploited to maximize returns and reduce the risk of poor drilling decisions. For such a workflow, we require a good log based TOC determination, followed by rock physics modelling, kerogen substitution and synthetic gather computation, from which characteristics of changes in the signal can be understood. Recasting log points into AI vs SI space then aids interpretation of a final inversion.

Method

We start our QI workflow for unconventional reservoirs with a robust determination of TOC concentration, achieved by combining the log based Passey method (1990) with a more recently derived theoretical version (Alfred and Vernik, 2012) that relates TOC to bulk density, using prior knowledge of the kerogen porosity. Here, we average the two TOC calculations, with greater weight given to the bulk density method when poor-quality core data is only available, or towards the Passey method where there is doubt about the validity of the kerogen porosity.

With a robust TOC log curve derived, the second step of our workflow uses the Alfred and Vernik (2012) model for representing an unconventional shale reservoir. This considers shale as a mixture of a hydrocarbon pore-filled organic phase, characterized using the kerogen volume which we derive from TOC values, and a water-filled inorganic phase. To this, we then apply the Vernik-Kachanov method (Vernik, 2016) to compute bulk density and bedding normal velocities. This uses the separate contributions that porosity and crack-like inclusions make to the kerogen and non-kerogen phases of the shale model, and enables density and velocity RPMs to be built (Figure 1) to aid with setting parameter values for the two phases.

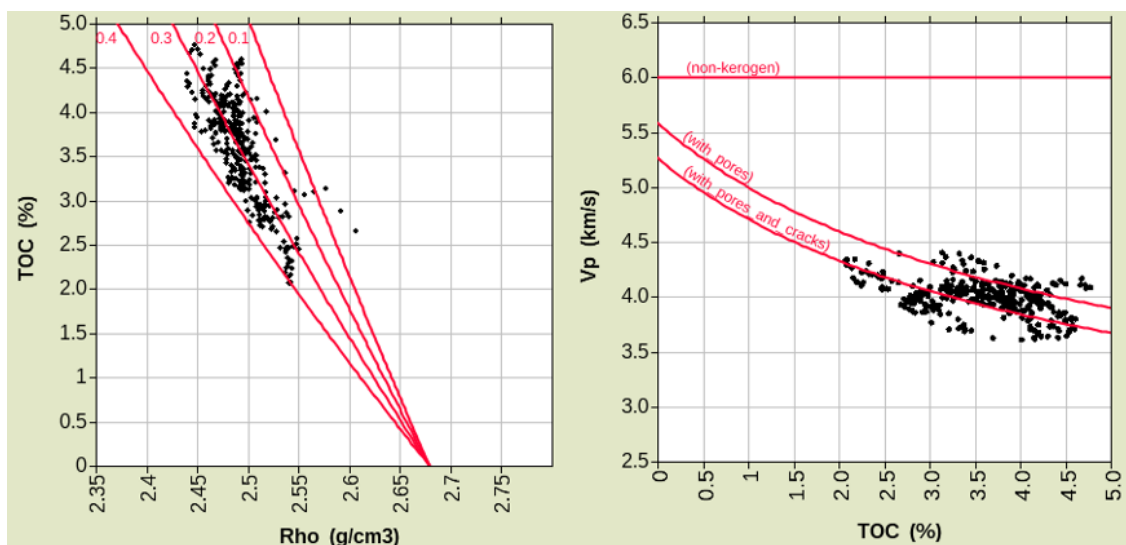


Figure 1 Rock physics models giving the relationship between TOC versus density (left) and versus Vp (right). The left RPM indicates that the predicted kerogen porosity for this well is 0.3.

The V_p versus TOC RPM (Figure 1, right) is constructed using the Vernik-Kachanov method, first computing the non-kerogen phase by mixing dry-clay, quartz and carbonate proportions to give a constant V_p (horizontal line along top of right cross-plot) and then adding water-filled pores to the non-kerogen phase before it is mixed with kerogen, whose porosity is assumed oil-wet. Cracks, parameterized by an effective-stress-dependent crack density factor, are added to the mixed phases, resulting in the lower curve which passes through the cloud of points.

The derivation of these RPMs allows forward modelling of V_p , V_s and density log curves, from which we compute synthetic gathers to show the impact that individual parameters have on the amplitude versus offset (AVO) signal of the seismic data. Because the shale exhibits a strong polar anisotropy, we use a Ruger (1998) based formulation to compute a reflectivity series, which is convolved with a wavelet extracted from the near stack seismic data, to compute gathers. The anisotropy is estimated from a derived empirical relationship for shale reservoirs (Vernik, 2016) that relates V_p to the epsilon parameter (Thomsen, 1986). Cross-plotting of Thomsen parameters, measured from cores, indicates that a 1:1 relationship between epsilon and gamma and a ratio of 2:1 between epsilon and delta in unconventional shale reservoirs is a suitable approximation to derive the full set of Thomsen parameters from epsilon (Vernik, 2016).

To test the sensitivity of the AVO response of the gathers to different TOC concentrations, we use kerogen substitution to perturb the velocity and density log curves and compute new sets of synthetics. The procedure is shown using a series of log curves in Figure 2. First, the TOC log values within our target formation are used as inputs to the RPMs that were set up above, and to forward model a set of theoretical density, V_p and V_s outputs (black curves in tracks 2 to 4). The TOC log is then perturbed, here by 50%, and the RPMs used again to forward model a new set outputs (purple curves in tracks 2 to 4).

Taking V_p as an example, the calculation is made from two forward modelled V_p values at each sample, V_{pTOC} (log TOC) and V_{pTOC50} (perturbed TOC), and computing the difference, $V_{pDifference}$:

$$V_{pDifference} = V_{pTOC50} - V_{pTOC}. \quad (1)$$

This output is applied to the original V_p log curve to give use a new curve, $V_{pSubstituted}$:

$$V_{pSubstituted} = V_{pLog} + V_{pDifference}. \quad (2)$$

A similar approach is applied to compute $V_{sSubstituted}$ and $Density_{Substituted}$ log curves.

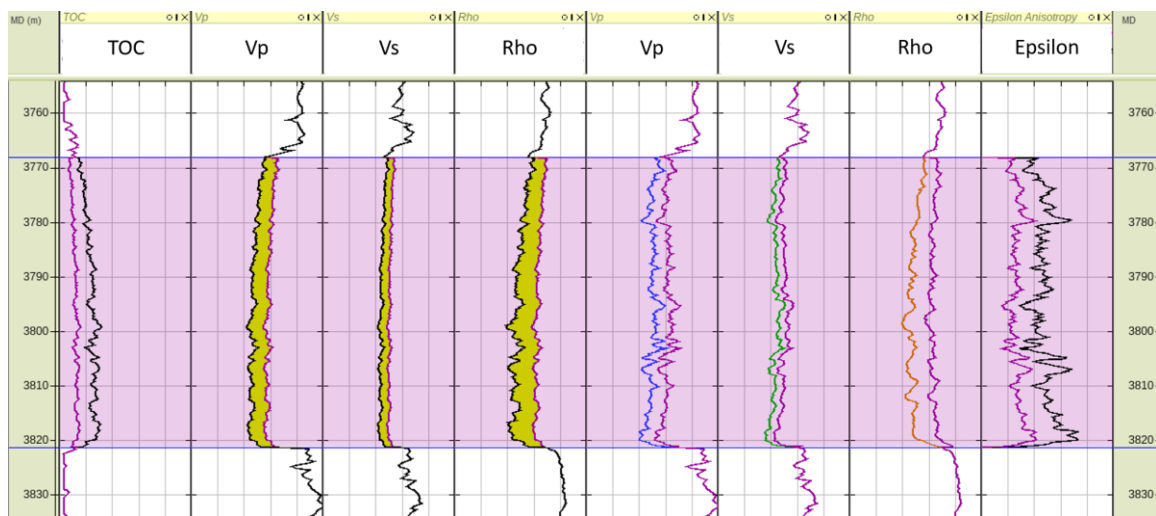


Figure 2 Measurement of TOC from well 1 (black, track 1) and its perturbed value (purple). Tracks 2 to 4 are the forward modelled outputs at original (black) and perturbed TOC (purple), equation (1). Tracks 5 to 7 show original log values (black) and following perturbation (purple), equation (2). Empirically derived epsilon is shown in track 8 from log (black) and substituted (purple) V_p values.

A replacement suite of Thomsen parameter log curves is also required from the substituted Vp log, which when calculated as described above, indicate a reduced anisotropy (track 8). We expect this since the substituted log curves contain less kerogen, which is a key anisotropy agent (Vernik, 2016).

The substitution of kerogen by the stiffer non-kerogen phase of the shale model has the effect of increasing the shale's density and velocities. This hardening is depicted in the RPMs in Figure 3, showing the points within the shale zone moving along their trend curves towards the lower TOC.

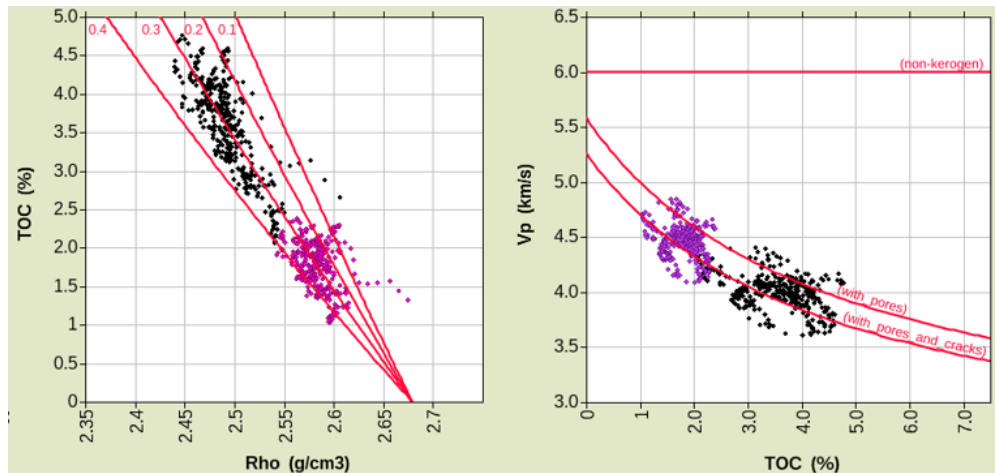


Figure 3 Cross-plots of TOC versus density (left) and TOC versus Vp (right) points from well 1 showing before (black) and after kerogen substitution (purple). Note how the substituted points shift along the RPM lines used in the forward modelling.

Kerogen substitution has been applied to well data from two separate producing formations that have different characteristics (Figure 4). The first well (left), used for the figures and discussion above, has a lower thermal maturity level and clay content than the second well (right). These observations, in addition to the higher effective stress in well 1, mean that a different parameterization is needed to compute well 2's RPMs. The two formations are encased within vertically heterogeneous overlaying formations with impedances greater than the shale.

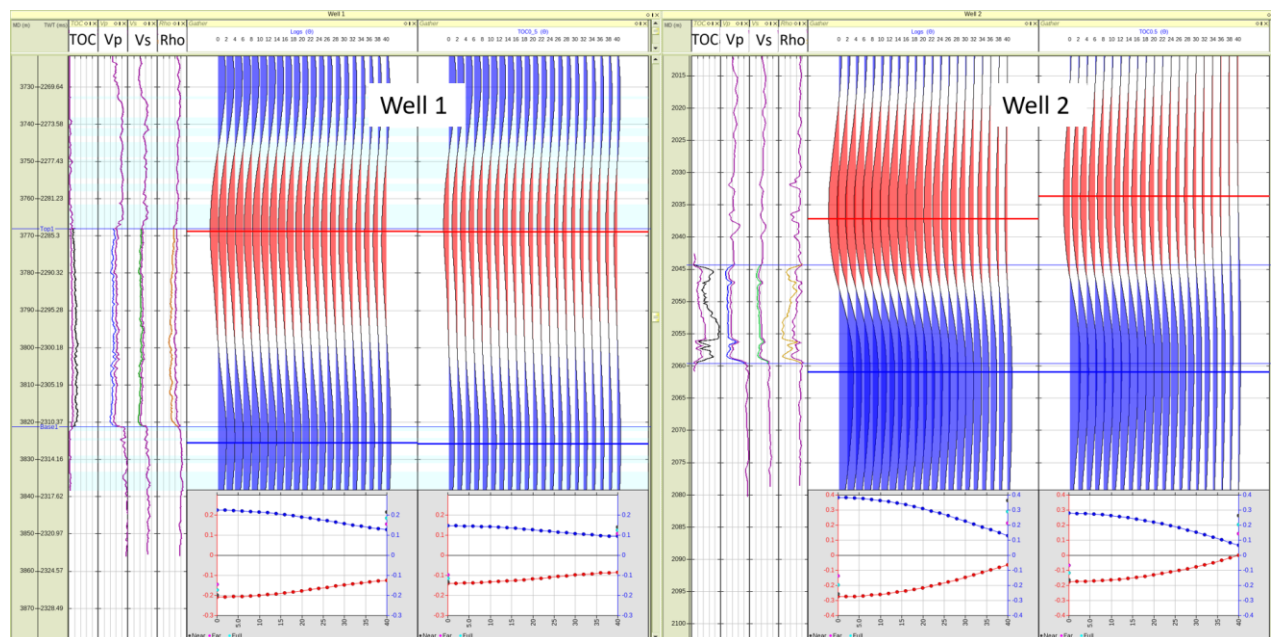


Figure 4 Log data (TOC, Vp, Vs and density, tracks 1 to 4), original synthetic gather (track 5) and gather computed following kerogen substitution (track 6) for well 1 (left) and well 2 (right). Tracks are plotted with the same scale and show, for example, that well 2 has higher TOC.

Both sets of gathers show a class IV AVO response, which is expected from having a lower impedance target encased within the harder surrounding material (see the V_p , V_s and density tracks in Figure 4). This is manifest in the left gather of each well, giving stronger negative and positive signals at the top and bottom of the shale target zone, and is quantified in the reflection coefficient versus angle of incidence plots at the base of each gather. With the kerogen content reduced by the substitution, the target zones' impedances harden (right gathers of each well) and the AVO signal decreases by some 40% for both wells.

Casting the points into AI vs SI space (Figure 5) indicates that it is possible to discriminate high TOC from lower TOC, and suggests that it would be worth investigating whether simultaneous inversion could map productive formations in the shale reservoir. Lower TOC values will map into higher values in the AI vs SI space, as shown by the movement of points following kerogen substitution.

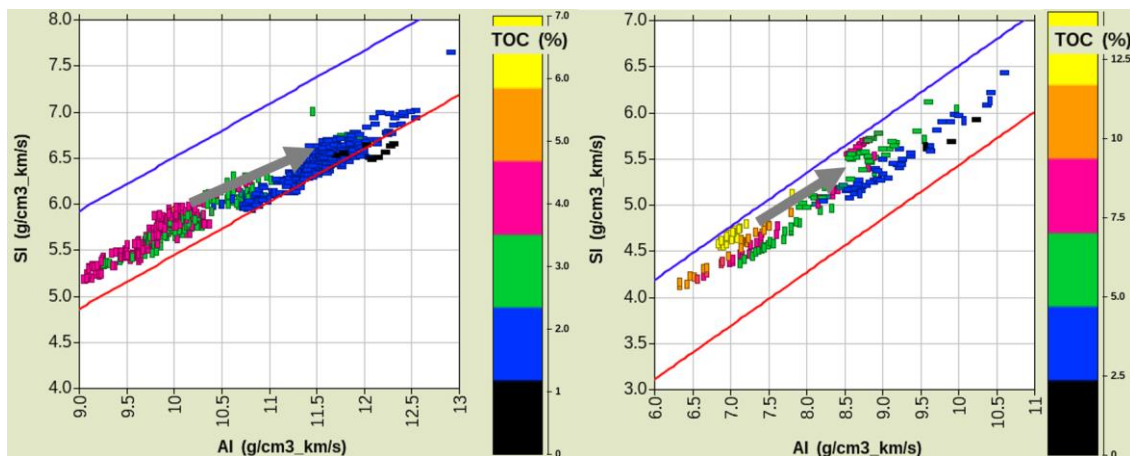


Figure 5 Cross plots of AI v SI for well 1 (left) and well 2, with points coloured by TOC (%) value. Original points are shown with vertical bars and following kerogen substitution with horizontal bars. The arrows indicate movement of points after substitution. Trend lines map AI to SI with a low TOC of 1% (red) and at maximum likely TOC of 14% (blue).

Conclusions

By using rock physics and the construction of a workflow, we have shown that quantitative interpretation is a viable proposition for making drilling decisions in unconventional reservoirs. Starting with the computation of a TOC log, followed by its use in rock physics modelling, the shale is parameterized in terms of hydrocarbon associated kerogen and non-kerogen components. The combination of kerogen substitution, together with forward modelling and cross-plotting, is valuable for understanding AVO and inversion outputs, similar to fluid substitution in conventional reservoirs. The discrimination within AI vs SI space of formations with higher TOC concentrations, indicative of higher hydrocarbon associated kerogen, is demonstrated.

References

- Alfred, D., and L. Vernik, 2012. A new petrophysical model for organic shales: 53rd Annual Logging Symposium, SPWLA conference paper 2012-217.
- Passy, Q.R., Creaney, S., Kulla, J.B., Moretti, F.J., and Stroud, J.D., 1990. A practical model for organic richness from porosity and resistivity logs: AAPG Bulletin, 74, 1777-1794.
- Ruger, A., 1998. Variation of P-wave reflectivity with offset and azimuth in anisotropic media. Geophysics, 63, 935-947.
- Simm, R., and Bacon, M., 2014. Seismic Amplitude, Cambridge.
- Thomsen, L., 1986. Weak elastic anisotropy. Geophysics, 51, 1954-1966.
- Vernik, L., 2016. Seismic Petrophysics in Quantitative Interpretation, 2nd Edition, SEG.